JACS
JOURNAL OF THE AMERICAN CHEMICAL SOCIETY
Article
pubs.acs.org/JACS

Asymmetric Growth in Polyelectrolyte Multilayers

Ramy A. Ghostine, Marie Z. Markarian, and Joseph B. Schlenoff*

Department of Chemistry and Biochemistry, The Florida State University, Tallahassee, Florida 32306-4390, United States

Supporting Information

ABSTRACT: Radioactive counterions were used to track the ratio of positive to negative polymer repeat units within a polyelectrolyte multilayer made from poly(diallyldimethylammonium chloride), PDADMAC, and poly(styrene sulfonate), PSS. For this widely employed pair of "linearly" assembled polyelectrolytes it was found that the accepted model of charge overcompensation for each layer is incorrect. In fact, overcompensation at the surface occurs only on the addition of the polycation, whereas PSS merely compensates the PDADMAC. After the assembly of about a dozen layers, excess positive sites begin to accrue in the multilayer. Treating the surface as a reaction−diffusion region for pairing of polymer charges, a model profile was constructed. It is shown that different reaction−diffusion ranges of positive and negative polyelectrolyte charge lead to a blanket of glassy, stoichiometric complex growing on top of a layer of rubbery, PDADMAC-rich complex. Though overcompensation and growth was highly asymmetric with respect to the layer number, entirely conventional "linear" assembly of the multilayer was observed. The impact of asymmetric growth on various properties of multilayers is discussed.

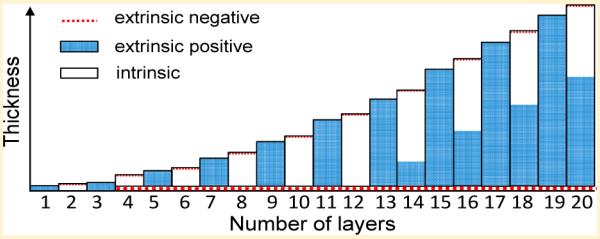

INTRODUCTION

Polyelectrolyte multilayers (PEMUs) are made by alternately exposing a substrate to solutions of oppositely charged polyelectrolytes.[1] Thousands of publications detail the myriad of applications for these extraordinarily versatile thin films. A sizable, though much smaller, body of work focuses on the fundamentals of multilayer assembly and behavior. It is now accepted that a critical feature of PEMU buildup is the reversal of surface charge, priming the surface for the next polyelectrolyte layer.[1a] Models for multilayer buildup show how excess polymer charge is located either near the surface[2] (for "linearly" growing systems) or throughout the film (for those systems that grow "exponentially").[3] As shown in Scheme 1, this excess charge pairs with incoming polyelectrolyte, releasing ions and water—an entropic driving force[4] for polyelectrolyte complex assembly at the surface.

Charge is balanced within these films of polyelectrolyte complex by a combination of polyelectrolyte repeat units and small counterions. Insight on multilayer buildup is gained by tracking polyelectrolytes and/or counterions, as stoichiometry in polyelectrolyte charge mirrors that of counterions; an excess of one polyelectrolyte must be accompanied by an equal excess of counterion. Models for PEMU growth, such as depicted in Scheme 1, show counterions at the surface, ready to be displaced by the next layer of incoming polyelectrolyte. In this particular representation, no ions are found in the bulk of the PEMU. Scheme 1 is oversimplified because it presents individual discrete layers of polymers, whereas each layer is believed to interpenetrate somewhat, creating a "fuzzy" band of material.[1a] Likewise, ions at the surface are assumed to be spread over a band.[2] When the importance of counterions in every physical property of multilayers began to be recognized, attempts were made to measure them. These efforts produced contradictory conclusions as to whether they were present in the bulk[5] or not.[2,6] In this controversy we have contradicted ourselves, finding them only at the surface[6c] and then also in the bulk.[7]

In the present work we measure both anions and cations during buildup of one of the most widely used pair of polyelectrolytes,[1b] poly(styrene sulfonate), PSS, and poly(diallyldimethylammonium chloride) PDADMAC. For stoichiometries close to 1:1 (i.e., stoichiometric) tracking the counterions is a more accurate method than tracking polyelectrolytes to discern whether there is a small excess of one polyelectrolyte. Charged dyes have been used to label counterion sites,[8] but they do not behave as small ions, especially with respect to diffusion, and they may be too large to access the entire multilayer. It is shown that the cartoon in Scheme 1 is wrong. Ions do not collect at the surface only, sometimes there are no surface ions, surface charge reversal does not occur symmetrically and is, in fact, not needed for completely conventional multilayer growth.

RESULTS AND DISCUSSION

Polyelectrolyte multilayers assembled from PDADMAC and PSS in solutions of defined [NaCl] are model systems for linearly growing PEMUs.[2,9] Figure 1 depicts the increase in dry thickness for such a PEMU grown from 0.10, 0.25, or 0.50 M NaCl. As with all multilayer assembly, a "layer" is actually a thickness increment rather than a well-defined slab of pure polymer deposited on the surface.[1a] Although the thickness increment for each layer quickly becomes constant ("linear" growth), slight to distinct upward curvature is seen for the first

Received: February 5, 2013
Published: May 14, 2013

   dx.doi.org/10.1021/ja401318m | J. Am. Chem. Soc. 2013, 135, 7636−7646

Scheme 1. Cartoon Showing the Accepted Model for Assembly of a "Linearly" Growing Multilayer, i.e., Where Each Layer Adds the Same Amount of Polymer.[1a] a

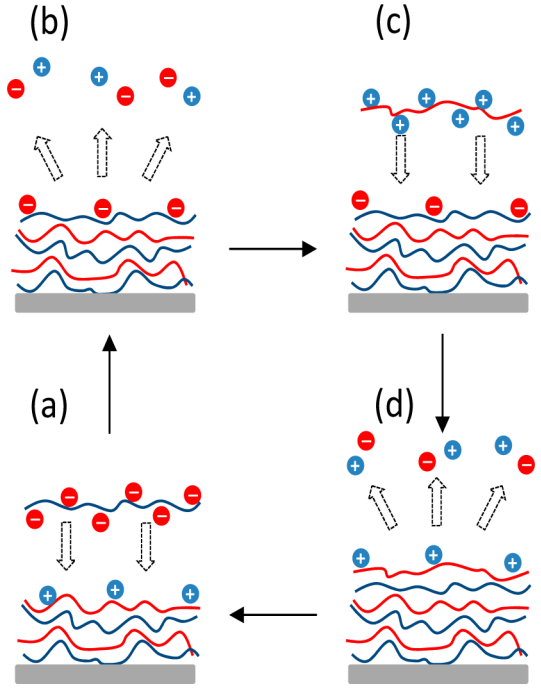

[a]Clockwise from bottom left: (a) excess polymer charge is balanced by cations (blue) on the PEMU surface or anions (red) on the incoming polyelectrolyte; (b) ions (and water molecules, not shown) are released when the incoming polyelectrolyte binds to the surface; and (c) and (d) the process repeats symmetrically to add the next layer etc.

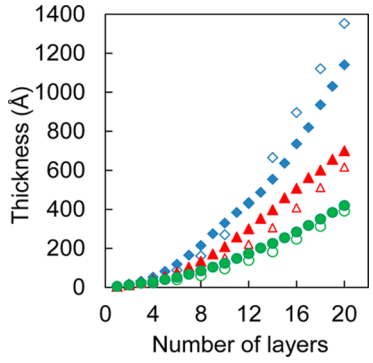

Figure 1. Thickness vs number of layers for PDADMA/PSS PEMUs built at 0.10 (●;○), 0.25 (▲;△), and 0.50 (◆;◇) M NaCl on Si wafer. Solid symbols represent the thicknesses measured by ellipsometry. Open symbols are thicknesses calculated from the sum of ion contents. Precision is ±3%, and accuracy is ±10%.

few layers—also a common feature of multilayer buildup. The fact that PEMUs build up faster at higher salt concentrations has been well known for some time.[1a] Thickness increases are seen for both positive and negative layers. In short, there is nothing in Figure 1 that appears to contradict the accepted mechanism in Scheme 1.

There is always concern that buildup history, such as sample manipulation during assembly, impacts the growth of a PEMU.[10] For example, our samples were subjected to drying, ion exchange, and counting as described later. A comparison was made between the buildup of PEMUs manipulated extensively, as in Figure 1, and those that were grown directly to the desired thickness without interruption (i.e., without drying between layers). As seen in Figure S1 there was no significant difference in buildup.

Ionic content of PEMUs. The ion content for the samples in Figure 1 was determined using radiolabeled counterions (see Figures S2 and S3 for details). As demonstrated previously,[6c] radiolabeled ions provide high precision and accuracy in quantitative analytical measurements on PEMUs. They are supplied with such high specific activity that precision on the order of fractions of a monolayer may be achieved for ultrathin films, such as PEMUs. The β particles emitted by the ^{35}S and ^{14}C isotopes have a range on the order of tens of μm in plastic, which means they are not absorbed by PEMUs of <0.2 μm thickness. ^{22}Na produces a positron, which annihilates immediately to yield γ radiation with a significantly longer range.

To remove liquid wetting the surface of the PEMU prior to counting, we employed a brute force method: liquid was "blasted" off the surface of the multilayer using a jet of nitrogen. Residual counts on the back of the wafer were wiped off manually with a cotton swab. This method proved quite effective and reproducible, leaving only 0.4 cps above background (4 cps) on the wafer.

Counterions are found wherever charge is not balanced by ion pairing between polyelectrolyte repeat units, whether in the bulk or at the surface of the PEMU. Exchange of unlabeled with labeled ions reveals this "extrinsic" charge, as depicted in Scheme 2.

Scheme 2. Internal Charge Balance in PEMUs Is Maintained by a Combination of Extrinsic Charge (Polymer/Counterion Pairs) and Intrinsic Charge (Polymer/Polymer Ion Pairs)[a]

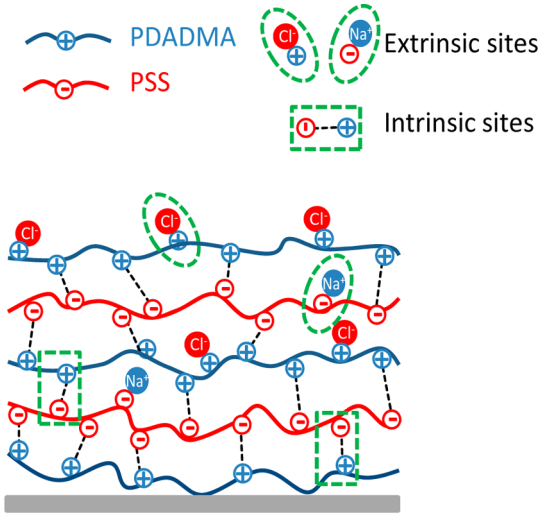

[a]Extrinsic charge is generically represented by Pol^+A^- and Pol^-C^+, and intrinsic charge by Pol^+Pol^-, where Pol^+, Pol^-, A^-, C^+ are, respectively, polycation and polyanion repeat units, counteranion, and counter-cation.

Solutions employed for radiolabel ion exchange were of low concentration (10^{-4} M) for two reasons. First, the lower the concentration, the higher the specific activity (Ci mol^{-1}) available, which yields higher count rates and better detection limits. Second, it was essential that the polymer charge was labeled without increasing ion content by doping. The doping

dx.doi.org/10.1021/ja401318m | J. Am. Chem. Soc. 2013, 135, 7636−7646

level, y, depends on the solution concentration. For example, in the case of NaCl at low concentration, the doping level is given by $y = 0.35[\mathrm{NaCl}]$.[11] In 10^{-4} M NaCl there is negligible doping ($y = 3.5 \times 10^{-5}$).

Radiolabeled ions served complementary roles: $^{35}SO_4^{2-}$ exchanged ions balancing all excess positive polymer charge or "positive sites" (each sulfate balances two $DADMA^+$ sites). PDADMA/PSS multilayers are permeable to SO_4^{2-} ion.[12] $^{22}Na^+$ was a label for all negative sites (SS^-). ^{14}C-TEA^+ was only able to access surface negative sites. After deposition of each layer the wafer was rinsed in water then immersed into a solution of radiolabeled ions. Excess solution was removed with a jet of N_2, and the sample counted. To demonstrate complete (i.e., equilibrium) exchange, counting after 5, 10, 15, 30, 60, 360, and 720 min exposure to radiolabeled ions was performed. For the thickest PEMUs, no change in count rate was observed after 15 min, which was thus chosen as the immersion time for all samples. An example of raw count rate (with 10 s gate time) is shown in Figure S5. The count rate spikes when the PMT is powered up but stabilizes after a few minutes. Typically, it took about 15 min to obtain a sufficient number of counts for good counting statistics (the counting error is the square root of the total number of counts).

Count rates were transformed into amounts with the aid of a calibration curve. Figure 2 depicts anion content as the molar

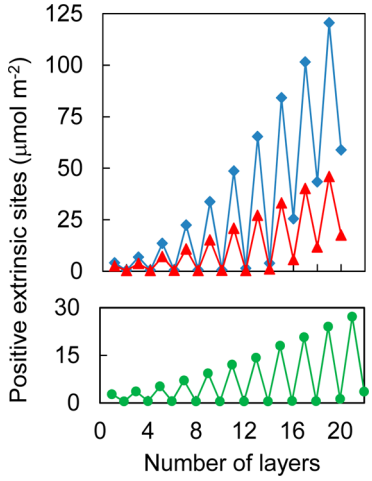

Figure 2. Positive bulk extrinsic sites (PDADMA*) for $(PDADMA/PSS)_n$ PEMUs, $n = 0-10$ built in 0.5 M (◆) and 0.25 M NaCl (▲); and $n = 0.5-11$ for 0.1 M NaCl (●). The extrinsic sites are radiolabeled with $^{35}SO_4^{2-}$ ion by ion exchange in 1×10^{-4} M $Na_2{}^{35}SO_4$ with a specific activity of 7.6 Ci mol^{-1}. The amounts of extrinsic sites are presented as areal density, or μmol m^{-2}. Precision is ±3%, and accuracy is ±5%.

coverage per m^2 (i.e., the areal density) for PEMU buildup from 0.10, 0.25, and 0.50 M NaCl. Anions label the extrinsic DADMA repeat units or "positive sites." Toward the beginning, all three curves show responses in accordance with the accepted model in Scheme 1. For odd layers, where PDADMA is the top layer, many positive sites are seen, consistent with a PEMU overcompensated with PDADMA. On the addition of PSS, all of these positive sites are consumed, also consistent with Scheme 1. The density of positive sites grows with each layer as the layer thickness grows, consistent with the initial upward curvature in Figure 1. After about 12–14 layers have been added, the data take an unexpected turn: the addition of PSS no longer compensates all the excess PDADMA charge. In other words, the PEMU contains anions at all times. The buildup reaches a "steady state," where the increase and decrease of positive sites are the same with respective PDADMA and PSS layers. However, the decrease is always slightly, but consistently, less than the increase. Points for layers 40 and 41 are shown in Figure S6.

When $^{22}Na^+$ is used to probe negative sites, the findings were also unexpected. Instead of an oscillating (up–down) response to each layer, where the signal rises with PSS layers and falls with PDADMA layers (the mirror image of Figure 2), far fewer negative sites were observed, and the population of Na^+ increased in a couple of steps then remained roughly constant (Figure 3). Points for layers 40 and 41 are shown in Figure S7. Such a response suggests negative sites are "frozen" into the multilayer and remain as the PEMU builds up.

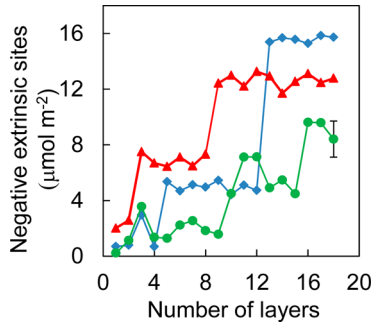

Figure 3. Negative bulk extrinsic sites density for $(PDADMA/PSS)_n$ PEMUs, $n = 0-10$, built from PSS and PDADMA solutions in 0.1 M NaCl (●), 0.25 M NaCl (▲), and 0.5 M NaCl (◆). Negative extrinsic sites (PSS*) are labeled with $^{22}Na^+$ by exchanging unlabeled ions in 1×10^{-4} M $^{22}NaCl$.

$^{22}Na^+$ is the ideal ion to probe the positive counterion content of PEMUs because it provides true self-exchange of unlabeled with labeled sodium ion. We also used a larger radiolabeled cation, ^{14}C-labeled tetraethylammonium, initially because we wished to employ a β-emitter, like the $^{35}SO_4^{2-}$ anion used to probe positive sites. It quickly became apparent that TEA^+, unlike $^{22}Na^+$, was not able to access the negative sites within the film, even after 12 h of immersion. In fact, the results in Figure 4 indicate that TEA^+ only exchanged with counterions at the surface negative sites. Limited penetration of a larger, hydrophobic ion is consistent with results of Liu and

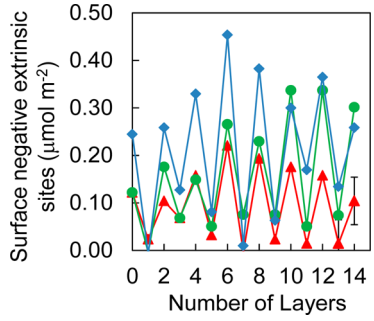

Figure 4. Surface negative extrinsic site density for $(PDADMA/PSS)_n$ PEMUs, $n = 0-7$, built from PSS and PDADMAC solutions in 0.1 M NaCl (●), 0.25 M NaCl (▲), and 0.5 M NaCl (◆). Surface ions were exchanged with radiolabeled $^{14}TEA^+$ by immersion in 1×10^{-4} M ^{14}C-TEABr with a specific activity of 5 Ci mol^{-1}.

dx.doi.org/10.1021/ja401318m | J. Am. Chem. Soc. 2013, 135, 7636–7646

Bruening, who observed strong selectivity against transport through a multilayer of molecules larger than 4−5 Å.[13] The ionic radii for Na^+, Cl^-, SO_4^{2-}, and TEA^+ are 1.1,[14] 1.7,[14] 2.3,[15] and 4.0[16] Å, respectively. Although the expected oscillation of surface charge with layer number was observed, the magnitude of the negative surface sites on a PSS layer was a small fraction (<1%) of the corresponding positive sites on a PDADMA layer. The straightforward conclusion is that, contrary to Scheme 1, PSS does not overcompensate the surface to a significant extent.

From Figure 4, the overcompensation level when PSS is the top layer is between 0.1 and 0.4 μmol m^{-2}, which is about 100 times less than overcompensation when PDADMA is the top layer. Assembly of this system is highly asymmetric with respect to the overcompensation, as it relies almost exclusively on overcompensation by the positive polyelectrolyte. Assuming a density of 1.1 g cm^{-3}, a monolayer of PSS repeat units is estimated to be about 4 μmol m^{-2}. Since there is <10% of a monolayer of Na^+ ions at the surface, it is quite possible that multilayering can proceed without switching the surface charge. Indeed, for the PDADMA/PSS system, Adusumilli and Bruening[17] observed, using streaming potential measurements, that multilayer assembly can proceed without surface charge reversal. In asymmetric buildup, multilayering can be driven by a change in, but not necessarily a reversal of, surface charge density.

Accurate and precise measurements of the total ion content permit estimates of the thickness increments for each layer. For example, Figures 2 and 3 show that almost all the overcompensation is provided by PDADMA and the PSS merely compensates, almost exactly, the excess PDADMA it can access. Using a density of 1.1 for the PDADMA/PSS ion pair, assuming three water molecules hydrate this ion pair at room temperature and 40% relative humidity[18] and including all the $PDADMA^+Cl^-$ (Figure 2) and PSS^-Na^+ extrinsic charges left behind (Figure 3), with a density of 1.1 g cm^{-3}, calculated thickness increments for each layer are shown in Figure 5. These are summed to give thicknesses of the PEMUs, as presented in Figure 1. Figure 5 is essentially the derivative of Figure 1. Agreement with the ellipsometric thickness is reasonable, considering the assumptions made. Importantly, thickness increments in the linear region (constant increments)

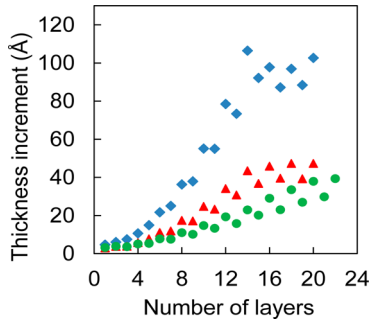

Figure 5. Thickness increment vs number of layers for PDADMA/PSS PEMUs built from 10 mM PSS and PDADMAC solutions in 0.1 M NaCl (●), 0.25 M NaCl (▲), and 0.5 M NaCl (◆). Increments were calculated from the amount of positive and negative extrinsic sites in Figures 2 and 3, taking the molecular weight of 1 pair of PDADMA/PSS 309 g mol^{-1} and the density 1.1 g mL^{-1}. Precision is ±3%, accuracy is ±10%.

match well. Figure S8 shows the thickness increments from ellipsometry.

For a full accounting of all charge during buildup, it was essential to verify that no polyelectrolyte was lost from the PEMU. Stripping of a polyelectrolyte from the surface by its oppositely charged partner has been demonstrated for strong mismatches in molecular weight.[19] Similarities between solution precipitated polyelectrolytes complexes and PEMUs have been emphasized throughout the development of the field.[20] "Soluble" complexes of mixed polyelectrolyte—actually colloidal dispersions—are observed for dilute systems when one polyelectrolyte is in large excess and their molecular weights differ substantially.[21] These suspensions of polyelectrolyte nanoparticles are stabilized by a shell of excess polymer charge.[22] Possible loss of polyelectrolyte from PEMU surfaces was explored using transmission IR spectroscopy on double-side polished wafers and the strong and distinctive SO_3^- band at around 1035 cm^{-1} (see Figure S9 for the IR spectra). Figure 6 shows that none of the PSS added is removed on exposure to

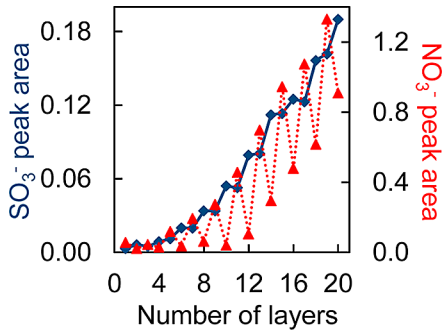

Figure 6. Sulfonate (1047−1022 cm^{-1}) and nitrate (1400−1272 cm^{-1}) FTIR peaks area vs number of layers during the buildup of 20 layers PDADMA/PSS on a double-side polished silicon wafer using 0.5 M $NaNO_3$ in the polyelectrolyte solutions. The dashed curve corresponds to the right *Y*-axis (NO_3^- peak area), and the solid curve corresponds to the left *Y*-axis (SO_3^-). All nitrate could be exchanged by immersing the PEMU in a solution of 10^{-4} M NaCl.

PDADMAC. The same result was observed with PDADMA (Figure S10). When buildup is carried out in 0.5 M $NaNO_3$, the positive sites are now labeled with infrared-active nitrate. Figure 6 shows the same oscillation in anion content as observed with Cl^- in Figure 2, i.e., all anions are expelled by the addition of a PSS layer until layer 12, where the population of excess positive sites builds up linearly (see Figure 6). The nitrate ions seen in Figure 6 may be exchanged with Cl^- by brief exposure to 10^{-4} M NaCl.

The change in stoichiometry of polyelectrolytes as the PEMU builds may be analyzed by examining the number of positive sites within the film after each layer is added. Specifically, the excess positive charge is defined as the fraction of overcompensation, y^+, of PDADMA compared to PSS:

$$y^+ = \frac{[\text{PDADMA}] - [\text{PSS}]}{[\text{PSS}]} \quad (1)$$

Figure 7 shows how the compensation on even (PSS) layers remains stoichiometric [PSS] = [PDADMA] until layer 12, 14, and 18 for buildup in 0.5, 0.25, and 0.10 M NaCl, respectively. Points beyond layer number 20 have been extrapolated using the thickness increments in Figure 5. These extrapolations are validated in Figures S6 and S7. With constant thickness

dx.doi.org/10.1021/ja401318m | J. Am. Chem. Soc. 2013, 135, 7636−7646

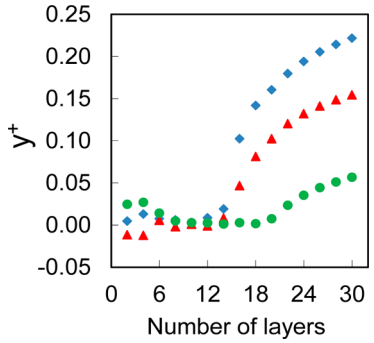

Figure 7. Fraction PDADMA overcompensation, y^+, when the multilayer is capped by PSS vs number of PSS layers in 0.1 (●), 0.25 (▲) and 0.5 M (◆) NaCl. Asymptotic residual extrinsic charge, y^+_∞, for PEMUs grown are 0.10, 0.21, and 0.30, respectively.

increment (linear growth) y^+ approaches a constant value y^+_∞ depending on the salt concentration. Respective values of y^+_∞ are 0.30, 0.21, and 0.10 for assembly from 0.5, 0.25, and 0.10 M NaCl. These are substantial and unexpected amounts of excess positive polyelectrolyte within the PEMU. Figure 8 depicts y^+

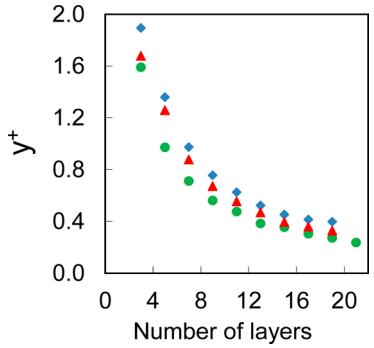

Figure 8. Overcompensation of PDADMA, y^+, when the multilayer is capped with PDADMA vs number of PDADMA layers in 0.1 (●), 0.25 (▲) and 0.5 M (◆) NaCl. Overcompensation approaches y^+_∞ for high layer number.

for PDADMA layers. A high degree of overcompensation is observed, especially toward the beginning of the PEMU buildup, and y^+ decreases with increasing layer number toward the same y^+_∞ values as in Figure 7.

It has become common practice to label nonlinear PEMU growth as "exponential." While initial upward curvature is seen in Figure 1, Figure 8 shows the growth at low layer number is not actually exponential. According to Lavalle et al.,[23] for exponential growth the concentration of PDADMAC* should remain constant with layer number. There is curvature because, for thin films, the substrate interferes with the PDADMA concentration profile (as seen in Scheme 3B). In the absence of demonstrated true exponential growth, the term "nonlinear" is more accurate than "exponential".

Near-Surface Chemical Composition by XPS. Although radiolabeled ions provide an accurate picture of charge balance within PEMUs, they do not reveal the locations of ions. The evidence thus far points to overcompensation, presumed to be at the surface, by PDADMA and, at the beginning, almost stoichiometric compensation by PSS. The surface composition of films at the start of the linear region of assembly from 0.50 M NaCl was determined by X-ray photoelectron spectroscopy (XPS) on 13- and 14-layer PEMUs. High-resolution XPS

Scheme 3. Model of Excess Positive and Negative Charge Profiles Through a PDADMA/PSS PEMU Built From 0.5M NaCl[a]

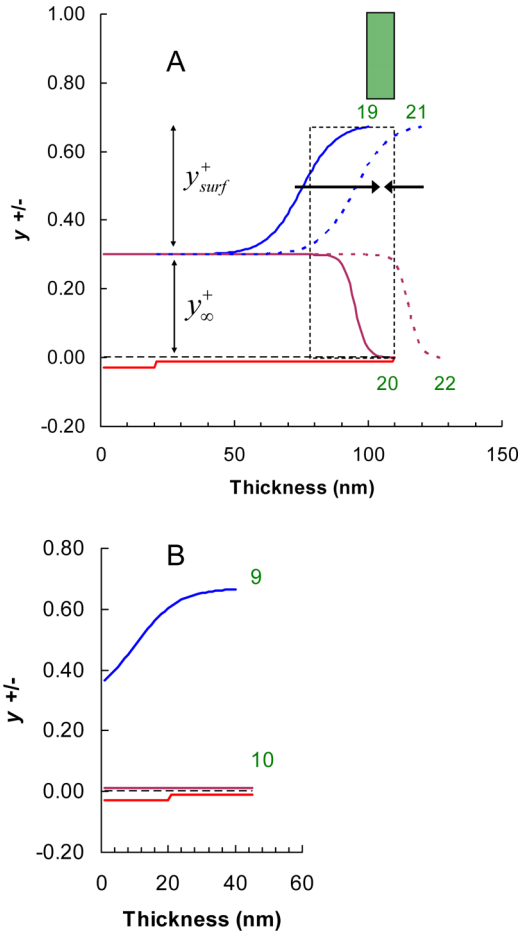

[a](A) Thicker films showing four consecutive "layers." (B) Thinner film showing two layers. The substrate is on the left at thickness = 0. Blue and purple lines are excess PDADMA (shown by $^{35}SO_4^{2-}$) for odd and even layers. The red line is excess PSS (shown by $^{22}Na^+$). There is almost no excess PSS. Note the asymmetry in the reaction–diffusion zone, dotted box, where PDADMA* travels further than PSS*. The thickness of the added layer of PSS is shown with a green bar. All positive (odd) layers leave the film with excess positive charge. For thin films, negative (even) layers remove this charge, but for thicker films positive charge remains in the bulk at all time. In this Scheme, values of 75, 95, 95, and 115 nm were used for $t_{1/2}$ and 15, 5, 15, and 5 nm for w in eqs 2 and 3, respectively for layers 19, 20, 21, and 22.

spectra were obtained for C (1s), N (1s), Cl (2p), S (2p), and Na (1s) photoelectrons at three takeoff angles, θ. Individual XPS spectra are presented in Figures S11 and S12. The surface was sampled at different depths, d, according to θ and the photoelectron energy: $d = 3\lambda \sin \theta$, where λ is the inelastic mean free path, estimated here from NIST database 71.

XPS data are summarized in Table 1, which shows element, layer number (13 or 14), takeoff angle, d, and the atom composition, i_x, normalizing to $i_C = 16$ from the atomic formula of the PDADMA/PSS ion pair ($C_8H_{16}N/C_8H_7SO_3$). The data are quite informative. S and N are unique to PSS and PDADMA, respectively. For the 13-layer film, excess N is observed at all depths probed, as summarized in Table 2. In contrast, the surface of the 14-layer (PSS terminated) film is

dx.doi.org/10.1021/ja401318m | J. Am. Chem. Soc. 2013, 135, 7636–7646

Table 1. Sampling Depth (d) and Relative Number of Atoms (i_x) for Different Elements, x, for $(PDADMA/PSS)_{6.5}$ (13 layers) and $(PDADMA/PSS)_7$ (14 layers) in 0.5 M NaCl at 15°, 45°, and 75° Take off Angles of XPS Analysis[a]

	takeoff angle								
	15°			45°			75°		
		i_x			i_x			i_x	
element x	D (nm)	13[b]	14[c]	d (nm)	13	14	d (nm)	13	14
C_{1s}	2.50	16.00	16.00	6.80	16.00	16.00	9.30	16.00	16.00
S_{2p}	2.70	0.57	1.09	7.40	0.70	1.02	10.10	0.67	1.02
N_{1s}	2.20	0.99	0.89	6.10	1.20	1.02	8.30	1.16	0.94
Cl_{2p}	2.60	0.16	0.01	7.20	0.26	0.00	9.90	0.18	0.00
Na_{1s}	0.80	0.11	0.15	2.10	0.22	0.22	2.90	0.18	0.18

[a]The sampling depths at each angle were calculated by the following equation: $d = 3\lambda \sin\theta$, where λ is the inelastic mean free path and θ is the take off angle. (Additional details are shown in Table S1). [b]13 layers. [c]14 layers.

Table 2. Atom Ratio of Sulfur to Nitrogen Using S_{2p} and N_{1s} for $(PDADMA/PSS)_{6.5}$ and $(PDADMA/PSS)_7$ in 0.5 M NaCl at 15°, 45°, and 75° Take off Angles of XPS Analysis

layer no.	θ (°)	S/N
	15	0.6
13	45	0.6
	75	0.6
	15	1.2
14	45	1.0
	75	1.1

stoichiometric in S and N. The proportions remain constant from about 3 to about 10 nm into the PEMU, showing that at least on the order of one "layer", there is no steep gradient in composition, in contrast with the exponential decay we proposed previously.[2] The fact that there is no observable change in S/N ratio for the PDADMA terminated film and that S is still observed at 3 nm, shows the PEMU surface is not a layer or blanket of PDADMA in loops and trains but is well mixed with PSS.

Counterions tell a similar story. Chloride is observed when PDADMA is on top, but they are gone when PSS is the last layer. A few sodium ions are seen irrespective of the top layer. A closer look reveals that there are fewer Cl^- than expected on the 13-layer film (0.3−0.4 ions would balance the excess PDADMA). Sodium is not expected on either surface, according to the results in Figure 4. We attribute the inconsistency in Na^+, and the lower-than-expected Cl^-, to partial loss of ions at the surface during the rapid rinse in water, e.g., by exchange with H^+, OH^-, or ions from dissolved CO_2, and to some contamination by Na^+ in the environment. Because S and N are unique to the polyelectrolytes, which are not washed or exchanged in this way, the atomic compositions for S and N are more accurate.

The Asymmetric Mechanism. Polyelectrolyte complexation is known to be a kinetically limited process, and PEMU formation, which is simply complexation within a thin film, is no exception.[20b,c] Salt ions are known to moderate the strength of polyelectrolyte ion pairing:[24] weaker interactions permit more mobility of polyelectrolytes within complexes.[25] The traditional explanation of "fuzzy" layering acknowledges limited interpenetration of polyelectrolyte components.[1a] Monolayer stratification (as shown for convenience in cartoons) does not occur. The classical mechanism must be revised to account for the asymmetry shown here, the surface composition and the residue of ions within the PEMU.

To align with mechanisms for bulk polyelectrolyte complexation, the addition of a new layer at the PEMU surface is best viewed as complexation of incoming (from solution) polyelectrolyte with whatever oppositely charged extrinsic polyelectrolyte sites within the PEMU can be accessed. Borrowing from the terminology of the Strasbourg group describing exponential growth,[3,23,26] polyelectrolyte "diffusing in" from solution complexes with polyelectrolyte "diffusing out" from some "reservoir" within the PEMU. The process is not simply diffusion but is also coupled with complexation. This is a type of reactive diffusion, well-known in mass transport. Our discussions and analysis are limited to "linear" growth only because this describes the behavior of PSS/PDADMA under the conditions in Figure 1. Porcel et al. addressed an "exponential" to linear transition with these diffusion arguments,[26a] as did Salomäki et al. in their analysis of the temperature effect on PDADMA/PSS buildup.[27]

Scheme 3, a representation of growth from 0.5 M NaCl, illustrates the reactive diffusion model with a cross-section through PEMUs with a high number of layers (i.e., in the linear regime) and with few layers (nonlinear growth). In Scheme 3 the profiles of excess charge of PDADMA (y^+) and PSS (y^-) are plotted. Scheme 3A models profiles of 4 consecutive layers starting from layer 19. All profiles in Scheme 3A show a constant excess of PDADMA, compensated by Cl^- ion (y^+_∞) within the bulk of about 0.3 consistent with Figures 7 and 8. Starting with layer 19, PDADMA-terminated, there is additional excess PDADMAC at the surface. Because the only information we have on this profile is the bulk excess (y^+_∞) and the surface excess (from the XPS results), we have represented the profile as sigmoidal with the function:

$$y_t^+ = y_\infty^+ + \frac{y_{surf}^+}{1 + 10^{t_{1/2} - t/w_1}} \quad (2)$$

for even layers and

$$y_t^+ = y_\infty^+ - \frac{y_\infty^+}{1 + 10^{t_{1/2} - t/w_2}} \quad (3)$$

for odd layers. There is only a slight negative charge at the surface for PSS layers and a small, constant population of SS^- in the first 20 or so nm.

The steepness of the profile is given by w, the midpoint by $t_{1/2}$ and y^+_{surf} is the excess (over bulk) at the PEMU/air interface. The model is consistent with the following observations: The first 10 nm of the film has approximately uniform composition (from the angular dependence of XPS, Table 1), and the

dx.doi.org/10.1021/ja401318m | J. Am. Chem. Soc. 2013, 135, 7636−7646

reaction-diffusion zone is about 40 nm thick. Similar schemes with similar profiles can be drawn for growth in 0.1 and 0.25 M NaCl but with respective y_{∞}^{+} values of 0.1 and 0.21.

What is the diffusing species? Stoichiometric PDADAMA/PSS complex is known to be in a glassy state at room temperature, where the polymer chains are "frozen" in place.[11] In a mechanism described previously,[25] counterions within the complex decouple the ion pairing between polyelectrolyte segments, facilitating local rearrangement of polymer (the mechanism is reproduced in Scheme S1). The diffusing species are thus counterion-compensated repeat units (i.e., extrinsic sites) which we label as PSS* and PDADMA* (for PEMU immersed in NaCl these would be PSSNa and PDADMAC). These "defects" travel throughout the complex. It is important to understand that defect diffusion does not require a specific polyelectrolyte repeat unit to travel long-range through bulk complex; a slight local rearrangement of polymers is enough to move this defect. It is also important to appreciate that counterions can move by hopping between defects.[7]

Ion and polymer motions are strongly influenced by water content[28] and by the presence of counterions.[11] Both plasticize the PEMU. At room temperature and with $[NaCl]_{aq} < 0.5M$, stoichiometric PSS/PDADMA is glassy.[11] Complex with excess PDADMA* is rubbery.[29] Asymmetric growth is driven by asymmetric reaction−diffusion lengths for PSS* and PDADMA*, where the latter diffuses further. Layer formation for both odd and even layers in Scheme 3 relies heavily on PDADMA* diffusion. For the addition of a PDADMA layer, PDADMA* diffuses through complex at the surface and overcompensates extensively.

Layer number 20 (PSS), provides key insight on the mechanism: PSS* diffuses in from solution and complexes with some of the PDADMA* within the film. The net directions of PSS* and PDADMA* are shown by the arrows, and the dotted box shows the reaction-diffusion zone for the complexation of these two species. As PSS* reacts with PDADMA* it creates a glassy, stoichiometric complex, which freezes the PSS in place. The reaction−diffusion range for PSS* through PSS/PDADMA is not far enough to consume all the PDADMA*, leaving some interior PDADMA* behind. In contrast, the reaction−diffusion range for PDADMA* through PSS/PDADMA is greater, so when layer 21 is sorbed it penetrates further into the film and overcompensates. Because PSS* is relatively immobile, a compact slab of deuterated PSS is found in multilayers employing neutron reflectivity to observe "fuzzy" layering within PEMUs.[1a]

For sufficiently thin films, such as <12 layers, in 0.5 M NaCl (Figure 1) the reaction−diffusion zone is thicker than the PEMU, as illustrated in Scheme 3, which allows PDADMA* to diffuse throughout the film and complex with PSS*. As a result, all the Cl^{-} counteranions are ejected from the PEMU when PSS* is added (Figure 2). Interestingly, the converse is not as complete. On the PDADMA layer one sees a large excess of PDADMA* (Figure 2) but a small amount of PSS* remains, as revealed by residual Na^{+} ions (Figure 3). Again, we believe the reason for this residual PSS* is related to its relatively poor mobility. The "reservoir" of PDADMA* which reacts with incoming PSS* is depleted by the substrate, on the left side in Scheme 4, leaving some unreacted PSS*.

While the mechanism is given in terms of defect mobilities, the polyelectrolyte repeat units are still part of a long chain which means there should be a molecular weight dependence on the mobility. Because PSS* is the rate-limiting reagent, there should be a stronger molecular weight dependence on layer thickness for PSS than for PDADMAC.

Scheme 4. Approximate Distribution of Positive (PDADMA*) and Negative (PSS*) Excess Polyelectrolyte Charge Following Each Layer during Buildup of a PSS/PDADMA Multilayer From 0.5 M NaCl[a]

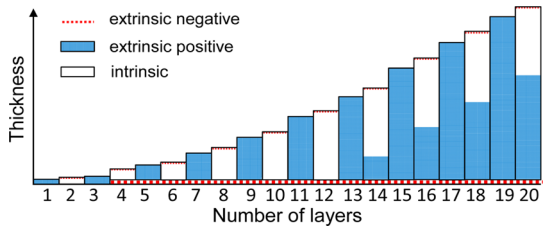

[a]The PEMU contains PDADMA* throughout the film following addition of all PDADMA "layers." The PSS adds to compensate all PDADMA* but does not overcompensate, providing only slight, if any, PSS* at the surface. When the film is thick enough, here about 14 layers, all PDADMA* is no longer accessed by incoming PSS, which leaves a growing layer of PDADMA* within the PEMU. A small population of PSS* remains trapped near the substrate. The concept of zones was proposed early in the study of multilayers to differentiate parts of the film that were next to the substrate, in the bulk and towards the surface. The scheme associates these zones with polyelectrolyte (and ion) stoichiometry.[1a,26a].

The product of the asymmetric growth mechanism is a very different kind of multilayer than is typically presented. Scheme 4 summarizes the locations of extrinsic and intrinsic polyelectrolyte as each layer is added. Toward the beginning of buildup, in the nonlinear region, the reaction-diffusion zone is thicker than the PEMU. Each PSS addition leaves an almost stoichiometric film (with all-intrinsic compensation), whereas each PDADMAC cycle produces a multilayer with excess PDADMA* throughout. After a sufficient number of layers (a number which depends on the salt concentration), a persistent layer of PDADMA* remains within the bulk of the film, and the alternation between extrinsic and intrinsic compensation continues only near the surface. The "blanket" of bulk PDADMA* grows.

Controversies and Consequences. With this new insight on PEMU buildup some of the persistent controversies on this topic may be addressed. A significant question is, with many contradictory answers so far, are there counterions within multilayers? The answer is that it depends. If the film is thin enough, there can be few ions within the film (for example, all the even layers up to 12 in Scheme 4) or the film can be full of ions (e.g., all the odd layers in Scheme 4). If one assumes that the ion content must be equal, one can be mislead by measuring only one of either positive or negative counterions. We have contradicted ourselves by first claiming there are no counterions within the bulk,[6c] then later finding that there are anions within PDADMA/PSS multilayers.[7] Unfortunately, the former conclusion was taken just before the exact point where extrinsic positive charge starts to persist (layer 22 for 0.1 M NaCl, Figure 2). The latter conclusion was made on much thicker films.

Many approaches to introducing extrinsic charge into PEMUs have been reported, including internal (de)protonation of weak acid polyelectrolytes,[8] thermal elimination of charged groups,[6c] redox charge injection,[6c,30] ion templating,[31] and high salt concentrations.[5h] The asymmetric mechanism results in

dx.doi.org/10.1021/ja401318m | J. Am. Chem. Soc. 2013, 135, 7636−7646

unanticipated extrinsic charge, which has several significant (unforeseen) practical consequences. Some examples follow.

Corrosion Protection. Multilayers have been shown to be effective in preventing or slowing corrosion of steel[32] and aluminum.[33] Chloride ions play an important role in corrosion. It is clear, from Scheme 4, that PDADMA/PSS multilayers terminated in PSS would only exclude chloride ions from contacting the surface of the metal if they were thin enough. Counterintuitively, thicker multilayers might actually perform worse than thinner ones in corrosion protection.

Reservoirs. Much effort is expended in creating reservoirs or layers of different materials within multilayers.[34] These reservoirs often contain bioactive materials. Scheme 4 shows that there is a reservoir for anions already built into the PDADMA/PSS PEMU. For thick films, this reservoir occupies most of the PEMU.

Sensors. If multilayers are used as coatings for sensors,[35] there will be preconcentration of negative species, whether desired or not, close to the surface.

Nanoreactors.[36] In an extension of the reservoir concept, nanoparticles have been produced by reducing metal ion salts within PEMUs.[37] These nanoparticles may be efficient catalysts (such as Pt^{o})[38] or they may have antimicrobial properties (such as Ag^{o}).[39] An unanticipated reservoir of anions within a PEMU can exchange with metal-containing anions concentrating them for reduction into metal particles. In this respect, complex anions of metals,[40,41] such as $Pt(Cl)_6^{2-}$ and $Au(Cl)_4^{-}$, would be taken up far more efficiently than bare cations, such as Ag^{+} and Cu^{2+}.

Mechanical Properties. The mechanical properties of multilayers have been examined extensively.[42] Much of the interest in the mechanical properties of biocompatible thin films, such as PEMUs, derives from the control offered over cell attachment and behavior,[43] such as the differentiation of stem cells.[44] Ion content strongly controls mechanical properties of complexes in PEMU and other morphologies. Complexes with extrinsic charge are much softer since counterions break ion pair cross-links between oppositely charged polyelectrolyte repeat units. For Scheme 4 the thicker PSS-terminated PEMUs essentially have a ~50 nm blanket of higher modulus stoichiometric complex on top of a layer of lower modulus nonstoichiometric complex. Although AFM nanoindentation measurements have shown a strong dependence of surface modulus on layer number, consistent with the asymmetric compensation mechanism, these measurements only probe the top 50 or so nanometers of the film. Thus, they do not provide whole-film properties, whereas buckling or deformation techniques would give a better average modulus of the entire film (for thick films)[45]

Protein Adsorption. At the bio/materials interface, multilayers have been used to control protein adsorption.[46] For example, PDADMA/PSS PEMUs terminated in PSS adsorb very little negative protein (such as albumin), whereas PDADMA-terminated multilayers are veritable sponges for the same protein.[47] Scheme 4 shows clearly the reason. For odd layers a large amount of anion is available to exchange with proteins, whereas even layers are glassy, ion-free surfaces which cannot sorb protein.

PEMU Hydration. Many studies have revealed a strong difference of water content in PDADMA/PSS multilayers depending on the terminating layer.[48] PDADMA-capped PEMUs are much more hydrated and swollen than their PSS-capped counterparts.[49] Scheme 4 again shows why. There are far more counterions in the bulk (for thin films less than 12 layers) or near the surface (for thick films more than 12 layers) when the PEMU is terminated with PDADMA. The osmotic pressure of these ions pulls in more water. The osmotic pressure of the extrinsic ions may be neutralized by adding a few atmospheres of osmotic stressor, such as poly(ethylene glycol), to the solution[50] or by physically pressing the water out.[51]

Membrane Flux. PEMUs have been used as selective membranes for separations, including nanofiltration[52] and chiral separations.[53] Ion permeability is a function of the diffusion coefficient and the concentration of ions within the multilayer. Excess polyelectrolyte yields persistent extrinsic charge, which includes or excludes ions via a classical Donnan mechanism. Extrinsic charge in stoichiometric multilayers may be introduced by doping with salt in solution. A multilayer containing a population of PDADMA* might show unexpectedly high permeability for anions and high selectivity for multiple over singly charged species. A specific example is provided below.

Ionic Content Controls PEMU's Permeability. Some years ago we started evaluating the mechanism of transport of electroactive ions, especially ferricyanide and ferrocyanide, through PDADMA/PSS.[7] Figure 9 shows the respective transport of these ions through a membrane covering a rotating disc electrode. The flux, as given by the current, of ferrocyanide through PDADMA/PSS (Figure 9B) followed a predicted trend: As the film thickness increased, the flux decreased continually. The ferrocyanide flux was higher when the PEMU was terminated with PDADMA, due, we reasoned, to ion inclusion of $Fe(CN)_6^{4-}$, by PDADMA* at the surface. There were, however, peculiar aspects to transport of the lower-charged ferricyanide. Figure 9 shows that flux initially decreases as the PEMU becomes thicker, but then the flux remains constant for PEMUs terminated with PSS. PDADMA-topped films presented little barrier to ferricyanide diffusion.

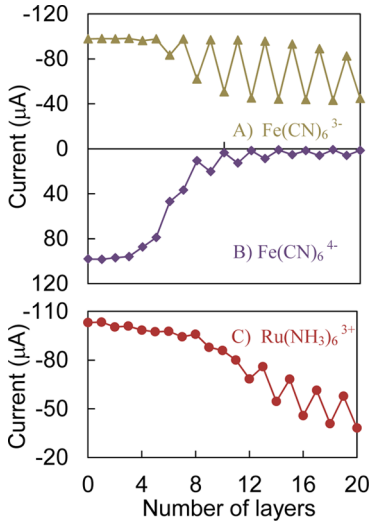

Figure 9. Limiting current at the rotating disk electrode vs number of layers for (A) 1 mM ferricyanide, (B) 1 mM ferrocyanide, and (C) 1 mM hexaaminеruthenium(III) chloride in 0.6 M NaCl; 20 mV/s sweep rate, rotation rate 1000 rpm, room temperature. Electrode area 0.1963 cm^2. PDADMA/PSS multilayers were built from 0.25 M NaCl. The residual [PDADMA*] of about $y_{\infty}^{+} = 0.21$ is enough to support ferricyanide hopping but not ferrocyanide transport.

dx.doi.org/10.1021/ja401318m | J. Am. Chem. Soc. 2013, 135, 7636−7646

The morphology represented in Scheme 4 helps to explain these results. The thickness of stoichiometric complex on top of the electrode only grows until about 12 layers, whereupon it rides as a 50 nm blanket on top of a layer of PDADMA*, which presents little barrier to the diffusion of $Fe(CN)_6^{3-}$. All odd (PDADMA) layers leave PDADMA* throughout the film, which readily transports ferricyanide, so the flux only slightly decreases for the thickest films.

The permeability of a positive ion through PDADMA/PSS also showed initially puzzling/contradictory behavior. The flux of $Ru(NH_3)_6^{3+}$ decreased with increasing film thickness, but the current for PSS-capped PEMUs was lower than that for previous or following films terminated in PDADMA. According to the classical view of multilayering, a layer of excess PSS at the surface should draw $Ru(NH_3)_6^{3+}$ in and enhance the flux. In fact, there is no excess PSS, only glassy, stoichiometric complex, which presents a greater barrier to $Ru(NH_3)_6^{3+}$ than the more hydrated PDADMA-terminated film.

Limits and Generality of Asymmetric Growth. In the present work, the ion content and buildup mechanism have been evaluated only for PEMUs from PSS and PDADMA. How general is the mechanism? In previous AFM nanoindentation studies we found a strong oscillation in surface mechanical properties in a PEMU made from polyelectrolytes quite different from those employed here: poly(allylamine hydrochloride), PAH, and poly(acrylic acid), PAA.[54] Both are weak acids/bases (though they were maintained fully ionized for our experiments) and both have a high charge density. Since mechanical properties are direct reporters of the extent of extrinsic charge, we concluded that the amount of overcompensation is also strongly asymmetric for that polyelectrolyte couple (again it was the polyanion, PAA, which yielded the most stoichiometric, glassy surface). In Figure S13, using $^{35}SO_4^{2-}$ as a label, we show that PAH/PAA buildup in 0.5 M NaCl has similar features to that of PDADMA/PSS; all positive extrinsic sites are removed on the addition of the PAA "layer" until about 24 layers, whereupon extrinsic positive sites start to build up. Labeling with $^{22}Na^+$ (Table S2) reveals fewer negative extrinsic sites throughout.

Because asymmetric growth is a consequence of differing reaction−diffusion distances for Pol^+A^- and Pol^-C^+ through Pol^+Pol^-, it is probably the rule rather than the exception, since it is highly unlikely that the two species will diffuse as far. At first glance, it would seem the easiest way to approach bulk stoichiometry in multilayers is to prepare them under conditions which minimize the distance Pol^+A^- and Pol^-C^+ must diffuse (e.g., using low, or no, salt during deposition (see Figures 2 and 5), which makes for rather lengthy assembly times. The start of linear growth (Figure 1) correlates with the number of layers at which positive extrinsic sites start to accumulate within the PSS-capped PEMU (Figure 4). This point could be termed the "intrinsic limit" for growth. It is interesting that this limit is not as much a function of the number of layers as it is the thickness. For example, from Figure 2 the intrinsic limit for growth in 0.1, 0.25, and 0.5 M NaCl is about 22, 16, and 14 layers, respectively, but the corresponding thickness for all three is about the same. Thus, to reach the maximum film thickness while maintaining bulk stoichiometry, it is actually more expedient to grow fewer layers with a higher salt concentration.

If the PEMU is plasticized by sufficient salt concentration, it goes through a glass transition, where the polymer mobility increases strongly.[11] For PSS/PDADMA at room temperature the glass transition occurs above about 1 M NaCl.[11] Figure 10 shows that some negative extrinsic sites actually start appearing on the surface of PSS/PDADMA when the salt concentration of the deposition solution is >1M. More PSS* also starts appearing in the bulk.

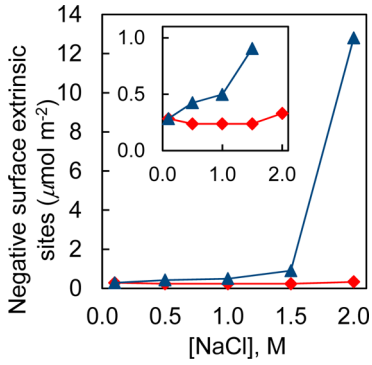

Figure 10. Negative surface extrinsic site density of $(PDADMA/PSS)_n$ PEMUs, n = 7.5 (◆, PDADMA terminated) and 8 (▲, PSS terminated) built from PSS and PDADMA solutions with various salt concentrations shown on the y-axis. The inset is a zoom-in. Surface sites were labeled with ^{14}C-TEA using 1×10^{-4} M ^{14}C-TEABr with specific activity 5 Ci mol^{-1}. No significant surface excess of PSS is seen, even with PSS as "top" layer, until the salt concentration reaches about 1.5 M. Precision is ±5%, and accuracy is ±10%.

CONCLUSION

If one polyelectrolyte does not remain static while the other adds to a PEMU, the concept of defined layers of material within a multilayer should be re-evaluated. It is probable that conclusions of fuzzy structure within the multilayer apply more to the polyanion, and observations of such structure are from fortuitous use and availability of deuterated PSS. There are also larger length scales of layering, where at least two zones of charge balance occur. The nature and extent of these zones depend on the last-added polyelectrolyte, where the polyanion yields a layer of glassy, stoichiometric complex. Such layering strongly influences the fundamental properties of multilayers. There are at least two key questions that remain to be answered. First, why does PDADMA* have a longer range than PSS*? Perhaps the chloride ion is a better plasticizer than Na^+. Second, what controls the degree of overcompensation of PDADMA*? While diffusion−reaction is a kinetic phenomenon, which severely limits the description of multilayer formation using thermodynamic (equilibrium) arguments, overcompensation may be an equilibrium property.

ASSOCIATED CONTENT

Supporting Information

Experimental details of multilayer buildup and radiolabeling, diagram of experimental setup, comparison of buildup with and without drying between layers, example of raw count rate vs number of layers, extended Figures 2 and 3, thickness increments from Figure 1, transmission FTIR using infrared-active nitrate ions, demonstration that no PDADMA is lost on layering, XPS spectra for 13 and 14 layers, mechanism for anion-assisted diffusion of PDADMA*, labeling of PAH/PAA during buildup. This information is available free of charge via the Internet at http://pubs.acs.org.

AUTHOR INFORMATION

Corresponding Author

schlen@chem.fsu.edu

Notes

The authors declare no competing financial interest.

ACKNOWLEDGMENTS

The authors gratefully acknowledge grants DMR-0939850 and DMR-1207188 from the National Science Foundation for supporting this work. We thank Dr. Eric Lochner for help with XPS measurements.

REFERENCES

(1) (a) Decher, G. *Science* **1997**, *277*, 1232−1237. (b) Decher, G.; Schlenoff, J. B. *Multilayer Thin Films: Sequential Assembly of Nanocomposite Materials*, 2nd ed.; Wiley-VCH: Weinheim, 2012.

(2) Schlenoff, J. B.; Dubas, S. T. *Macromolecules* **2001**, *34*, 592−598.

(3) Picart, C.; Mutterer, J.; Richert, L.; Luo, Y.; Prestwich, G. D.; Schaaf, P.; Voegel, J. C.; Lavalle, P. *Proc. Natl. Acad. Sci. U.S.A.* **2002**, *99*, 12531−12535.

(4) (a) Michaels, A. S. *J. Ind. Eng. Chem.* **1965**, *57*, 32−40. (b) Bucur, C. B.; Sui, Z.; Schlenoff, J. B. *J. Am. Chem. Soc.* **2006**, *128*, 13690−13691.

(5) (a) Schmitt, J.; Grünewald, T.; Decher, G.; Pershan, P. S.; Kjaer, K.; Lösche, M. *Macromolecules* **1993**, *26*, 7058−7063. (b) Kellogg, G. J.; Mayes, A. M.; Stockton, W. B.; Ferreira, M.; Rubner, M. F.; Satija, S. K. *Langmuir* **1996**, *12*, 5109−5113. (c) Lösche, M.; Schmitt, J.; Decher, G.; Bouwman, W. G.; Kjaer, K. *Macromolecules* **1998**, *31*, 8893−8906. (d) Caruso, F.; Lichtenfeld, H.; Donath, E.; Möhwald, H. *Macromolecules* **1999**, *32*, 2317−2328. (e) Ladam, G.; Schaad, P.; Voegel, J. C.; Schaaf, P.; Decher, G.; Cuisinier, F. *Langmuir* **2000**, *16*, 1249−1255. (f) Jaber, J. A.; Schlenoff, J. B. *Langmuir* **2007**, *23*, 896−901. (g) Tanchak, O. M.; Yager, K. G.; Fritzsche, H.; Harroun, T.; Katsaras, J.; Barrett, C. J. *J. Chem. Phys.* **2008**, *129*, 084901. (h) Guzmán, E.; Ritacco, H.; Rubio, J. E. F.; Rubio, R. G.; Ortega, F. *Soft Matter* **2009**, *5*, 2130−2142. (i) Zan, X. J.; Hoagland, D. A.; Wang, T.; Su, Z. H. *Macromolecules* **2012**, *45*, 8805−8812. (j) Riegler, H.; Essler, F. *Langmuir* **2002**, *18*, 6694−6698. (k) Hoogeveen, N. G.; Stuart, M. A. C.; Fleer, G. J.; Böhmer, M. R. *Langmuir* **1996**, *12*, 3675−3681.

(6) (a) Sukhorukov, G. B.; Schmitt, J.; Decher, G. *Ber. Bunsen-Ges.* **1996**, *100*, 948−953. (b) Laurent, D.; Schlenoff, J. B. *Langmuir* **1997**, *13*, 1552−1557. (c) Schlenoff, J. B.; Ly, H.; Li, M. *J. Am. Chem. Soc.* **1998**, *120*, 7626−7634. (d) Dubas, S. T.; Schlenoff, J. B. *Macromolecules* **2001**, *34*, 3736−3740. (e) Lourenco, J. M. C.; Ribeiro, P. A.; do Rego, A. M. B.; Fernandes, F. M. B.; Moutinho, A. M. C.; Raposo, M. *Langmuir* **2004**, *20*, 8103−8109.

(7) Farhat, T. R.; Schlenoff, J. B. *J. Am. Chem. Soc.* **2003**, *125*, 4627−4636.

(8) Chung, A. J.; Rubner, M. F. *Langmuir* **2002**, *18*, 1176−1183.

(9) Bertrand, P.; Jonas, A.; Laschewsky, A.; Legras, R. *Macromol. Rapid Commun.* **2000**, *21*, 319−348.

(10) Lvov, Y.; Ariga, K.; Onda, M.; Ichinose, I.; Kunitake, T. *Colloids Surf., A* **1999**, *146*, 337−346.

(11) Shamoun, R. F.; Hariri, H. H.; Ghostine, R. A.; Schlenoff, J. B. *Macromolecules* **2012**, *45*, 9759−9767.

(12) Malaisamy, R.; Bruening, M. L. *Langmuir* **2005**, *21*, 10587−10592.

(13) Liu, X. Y.; Bruening, M. L. *Chem. Mater.* **2004**, *16*, 351−357.

(14) Shannon, R. D. *Acta Crystallogr., Sect. A* **1976**, *A32*, 751−767.

(15) Waddington, T. C. *Adv. Inorg. Chem.* **1959**, *1*, 157−221.

(16) Robinson, R. A.; Stokes, R. H. *Electrolyte solutions; the measurement and interpretation of conductance, chemical potential, and diffusion in solutions of simple electrolytes*; 2d ed.; Butterworths: London, 1959.

(17) Adusumilli, M.; Bruening, M. L. *Langmuir* **2009**, *25*, 7478−7485.

(18) Farhat, T.; Yassin, G.; Dubas, S. T.; Schlenoff, J. B. *Langmuir* **1999**, *15*, 6621−6623.

(19) Sui, Z. J.; Salloum, D.; Schlenoff, J. B. *Langmuir* **2003**, *19*, 2491−2495.

(20) (a) Kovačević, D.; van der Burgh, S.; de Keizer, A.; Cohen Stuart, M. A. *Langmuir* **2002**, *18*, 5607−5612. (b) Sukhishvili, S. A.; Kharlampieva, E.; Izumrudov, V. *Macromolecules* **2006**, *39*, 8873−8881. (c) Xu, L.; Pristinski, D.; Zhuk, A.; Stoddart, C.; Ankner, J. F.; Sukhishvili, S. A. *Macromolecules* **2012**, *45*, 3892−3901.

(21) Dautzenberg, H.; Jaeger, W.; Kötz, J.; Philipp, B.; Seidel, C. H.; Stscherbina, D. *Polyelectrolytes: Formation, Characterization and Applications*; Hanser: Munich, 1994.

(22) Dautzenberg, H.; Hartmann, J.; Grunewald, S.; Brand, F. *Ber. Bunsen-Ges.* **1996**, *100*, 1024−1032.

(23) Lavalle, P.; Picart, C.; Mutterer, J.; Gergely, C.; Reiss, H.; Voegel, J. C.; Senger, B.; Schaaf, P. *J. Phys. Chem. B* **2004**, *108*, 635−648.

(24) Dautzenberg, H. *Macromolecules* **1997**, *30*, 7810−7815.

(25) Jomaa, H. W.; Schlenoff, J. B. *Macromolecules* **2005**, *38*, 8473−8480.

(26) (a) Porcel, C.; Lavalle, P.; Ball, V.; Decher, G.; Senger, B.; Voegel, J. C.; Schaaf, P. *Langmuir* **2006**, *22*, 4376−4383. (b) Lavalle, P.; Gergely, C.; Cuisinier, F. J. G.; Decher, G.; Schaaf, P.; Voegel, J. C.; Picart, C. *Macromolecules* **2002**, *35*, 4458−4465.

(27) Salomäki, M.; Vinokurov, I. A.; Kankare, J. *Langmuir* **2005**, *21*, 11232−11240.

(28) Hariri, H. H.; Lehaf, A. M.; Schlenoff, J. B. *Macromolecules* **2012**, *45*, 9364−9372.

(29) Lehaf, A. M.; Hariri, H. H.; Schlenoff, J. B. *Langmuir* **2012**, *28*, 6348−6355.

(30) Tagliazucchi, M.; Williams, F. J.; Calvo, E. J. *J. Phys. Chem. B* **2007**, *111*, 8105−8113.

(31) Balachandra, A. M.; Dai, J. H.; Bruening, M. L. *Macromolecules* **2002**, *35*, 3171−3178.

(32) (a) Farhat, T. R.; Schlenoff, J. B. *Electrochem. Solid-State Lett.* **2002**, *5*, B13−B15. (b) Shchukin, D. G.; Zheludkevich, M.; Yasakau, K.; Lamaka, S.; Ferreira, M. G. S.; Möhwald, H. *Adv. Mater.* **2006**, *18*, 1672−1678.

(33) Dai, J. H.; Sullivan, D. M.; Bruening, M. L. *Ind. Eng. Chem. Res.* **2000**, *39*, 3528−3535.

(34) (a) Boudou, T.; Crouzier, T.; Ren, K. F.; Blin, G.; Picart, C. *Adv. Mater.* **2010**, *22*, 441−467. (b) Wang, X. F.; Ji, J. *Langmuir* **2009**, *25*, 11664−11671. (c) Michel, A.; Izquierdo, A.; Decher, G.; Voegel, J. C.; Schaaf, P.; Ball, V. *Langmuir* **2005**, *21*, 7854−7859. (d) Luan, Y.; Ramos, L. *J. Am. Chem. Soc.* **2007**, *129*, 14619−14624. (e) Ji, Q.; Miyahara, M.; Hill, J. P.; Acharya, S.; Vinu, A.; Yoon, S. B.; Yu, J. S.; Sakamoto, K.; Ariga, K. *J. Am. Chem. Soc.* **2008**, *130*, 2376−2377.

(35) (a) DeLongchamp, D. M.; Hammond, P. T. *Chem. Mater.* **2003**, *15*, 1165−1173. (b) Araujo, I. M. S.; Zampa, M. F.; Moura, J. B.; dos Santos, J. R.; Eaton, P.; Zucolotto, V.; Veras, L. M. C.; de Paula, R. C. M.; Feitosa, J. P. A.; Leite, J. R. S. A.; Eiras, C. *Mater. Sci. Eng., C* **2012**, *32*, 1588−1593. (c) Evtugyn, G. A.; Hianik, T. *Current Analytical Chemistry* **2011**, *7*, 8−34. (d) Du, Y.; Chen, C. G.; Li, B. L.; Zhou, M.; Wang, E. K.; Dong, S. J. *Biosens. Bioelectron.* **2010**, *25*, 1902−1907. (e) Shi, H. B.; Song, Z.; Huang, J. D.; Yang, Y.; Zhao, Z. X.; Anzai, J. I.; Osa, T.; Chen, Q. *Sens. Actuators, B* **2005**, *109*, 341−347.

(36) Joly, S.; Kane, R.; Radzilowski, L.; Wang, T.; Wu, A.; Cohen, R. E.; Thomas, E. L.; Rubner, M. F. *Langmuir* **2000**, *16*, 1354−1359.

(37) (a) Kidambi, S.; Dai, J. H.; Li, J.; Bruening, M. L. *J. Am. Chem. Soc.* **2004**, *126*, 2658−2659. (b) Yang, G. B.; Chen, X. H.; Zhang, Z. M.; Song, S. Y.; Yu, L. G.; Zhang, P. Y. *Lubr. Sci.* **2012**, *24*, 313−323. (c) Zan, X. J.; Su, Z. H. *Langmuir* **2009**, *25*, 12355−12360. (d) Logar, M.; Jančar, B.; Suvorov, D.; Kostanjšek, R. *Nanotechnology* **2007**, 18.

(38) Bhattacharjee, S.; Dotzauer, D. M.; Bruening, M. L. *J. Am. Chem. Soc.* **2009**, *131*, 3601−3610.

(39) Grunlan, J. C.; Choi, J. K.; Lin, A. *Biomacromolecules* **2005**, *6*, 1149−1153.

(40) (a) Farhat, T. R.; Hammond, P. T. *Chem. Mater.* **2006**, *18*, 41−49. (b) Markarian, M. Z.; El Harakeh, M.; Halaoui, L. I. *J. Phys. Chem. B* **2005**, *109*, 11616−11621.
(41) (a) Chen, H. J.; Dong, S. J. *Talanta* **2007**, *71*, 1752−1756. (b) Santos, H. A.; Chirea, M.; Garcia-Morales, V.; Silva, F.; Manzanares, J. A.; Kontturi, K. *J. Phys. Chem. B* **2005**, *109*, 20105−20114.
(42) (a) Nolte, A. J.; Cohen, R. E.; Rubner, M. F. *Macromolecules* **2006**, *39*, 4841−4847. (b) Heuvingh, J.; Zappa, M.; Fery, A. *Langmuir* **2005**, *21*, 3165−3171. (c) Lutkenhaus, J. L.; Hrabak, K. D.; McEnnis, K.; Hammond, P. T. *J. Am. Chem. Soc.* **2005**, *127*, 17228−17234. (d) Han, L.; Wang, L. F.; Chia, K. K.; Cohen, R. E.; Rubner, M. F.; Boyce, M. C.; Ortiz, C. *Adv. Mater.* **2011**, *23*, 4667−4673.
(43) (a) Gribova, V.; Auzely-Velty, R.; Picart, C. *Chem. Mater.* **2012**, *24*, 854−869. (b) Engler, A. J.; Richert, L.; Wong, J. Y.; Picart, C.; Discher, D. E. *Surf. Sci.* **2004**, *570*, 142−154. (c) Richert, L.; Boulmedais, F.; Lavalle, P.; Mutterer, J.; Ferreux, E.; Decher, G.; Schaaf, P.; Voegel, J. C.; Picart, C. *Biomacromolecules* **2004**, *5*, 284−294.
(44) (a) Moby, V.; Labrude, P.; Kadi, A.; Bordenave, L.; Stoltz, J. F.; Menu, P. *J. Biomed. Mater. Res., Part A* **2011**, *96A*, 313−319. (b) Veerabadran, N. G.; Goli, P. L.; Stewart-Clark, S. S.; Lvov, Y. M.; Mills, D. K. *Macromol. Biosci.* **2007**, *7*, 877−882. (c) Semenov, O. V.; Malek, A.; Bittermann, A. G.; Vörös, J.; Zisch, A. H. *Tissue Eng., Part A* **2009**, *15*, 2977−2990.
(45) (a) Schweikart, A.; Horn, A.; Boker, A.; Fery, A. *Complex Macromol. Syst. I* **2010**, *227*, 75−99. (b) Hendricks, T. R.; Lee, I. *Nano Lett.* **2007**, *7*, 372−379. (c) Nolte, A. J.; Rubner, M. F.; Cohen, R. E. *Macromolecules* **2005**, *38*, 5367−5370.
(46) (a) Wong, S. Y.; Han, L.; Timachova, K.; Veselinovic, J.; Hyder, M. N.; Ortiz, C.; Klibanov, A. M.; Hammond, P. T. *Biomacromolecules* **2012**, *13*, 719−726. (b) Vogt, C.; Ball, V.; Mutterer, J.; Schaaf, P.; Voegel, J. C.; Senger, B.; Lavalle, P. *J. Phys. Chem. B* **2012**, *116*, 5269−5278. (c) Ladam, G.; Schaaf, P.; Decher, G.; Voegel, J. C.; Cuisinier, F. J. G. *Biomolecular Engineering* **2002**, *19*, 273−280.
(47) Salloum, D. S.; Schlenoff, J. B. *Biomacromolecules* **2004**, *5*, 1089−1096.
(48) Carrière, D.; Krastev, R.; Schönhoff, M. *Langmuir* **2004**, *20*, 11465−11472.
(49) Ramos, J. J. I.; Stahl, S.; Richter, R. P.; Moya, S. E. *Macromolecules* **2010**, *43*, 9063−9070.
(50) Schlenoff, J. B.; Rmaile, A. H.; Bucur, C. B. *J. Am. Chem. Soc.* **2008**, *130*, 13589−13597.
(51) de Vos, W. M.; Mears, L. L. E.; Richardson, R. M.; Cosgrove, T.; Barker, R.; Prescott, S. W. *Macromolecules* **2013**, *46*, 1027−1034.
(52) (a) Su, B. W.; Wang, T. T.; Wang, Z. W.; Gao, X. L.; Gao, C. J. *J. Membr. Sci.* **2012**, *423*, 324−331. (b) Lu, O. Y.; Malaisamy, R.; Bruening, M. L. *J. Membr. Sci.* **2008**, *310*, 76−84.
(53) Rmaile, H. H.; Schlenoff, J. B. *J. Am. Chem. Soc.* **2003**, *125*, 6602−6603.
(54) Lehaf, A. M.; Moussallem, M. D.; Schlenoff, J. B. *Langmuir* **2011**, *27*, 4756−4763.